Water-stable perovskite-on-polymer fluorescent microspheres for simultaneous monitoring of pH, urea and urease

Jia An[a, b], Meizhu Chen[a], Guoyi Liu [a, b], Yongqin Hu[a, b], Rubing Chen[a], Ying Lyu[a], Sanjiv Sharma[c], and Yufei Liu[a, b, c *]

[a] Key Laboratory of Optoelectronic Technology & Systems (Chongqing University), Ministry of Education, Chongqing 400044, China

[b] Collaborative Innovation Center for Brain Science, Chongqing University, Chongqing 400044, China

[c] Centre for NanoHealth, College of Engineering, Swansea University, Singleton Park, Swansea SA2 8PP, UK

[*]To whom correspondence should be addressed

Key Laboratory of Optoelectronic Technology & Systems (Chongqing University), Ministry of Education, Chongqing 400044, China

ORCID: 0000-0003-2988-8843

Tel: +86 13522636676

E-mail address: Yufei.Liu@cqu.edu.cn

Abstract

Perovskite materials have attracted attention due to their excellent optical and electrical properties, however, their unsatisfactory stability limits their application in biochemical detection. In this paper, $CsPbBr_3$ perovskite quantum dots were successfully encapsulated in poly (styrene/acrylamide) microspheres, using a swelling–shrinking method. The manufactured perovskite microspheres (PDPS composites) not only maintained strong photoluminescence (PL) stability but also demonstrated great water solubility. Additionally, a real-time pH monitoring platform was constructed based on the prepared PDPS composites and dopamine, and the system showed a good linear relationship in a pH range of 4-12. Furthermore, urea could be hydrolyzed to produce hydroxyl groups, thereby increasing the pH of the solution. Therefore, this system was then extended for urea and urease detection. As a result, the detection limits of urea and urease were recorded as 1.67 μM and 2.1 mU/mL, respectively. This development provides an interesting demonstration of the expanding list of applications of perovskite materials.

Abbreviations: PDPS - perovskite microspheres

KEY WORDS: Perovskite quantum dots, PS-PAA microspheres, pH sensing, Urea/Urease monitoring

1 Introduction

A material with the chemical formula ABO_3 is commonly referred to as perovskite [1]. First synthesized in 2015 [2], $CsPbX_3$ perovskite quantum dots materials have been extended for a plethora of wide range of applications due to their fantastic optical properties. These properties mainly include a very high quantum yield (nearly 100%), tunable emission, and narrow emission width [3-5]. However, due to their sensitivity to humidity, light, and temperature, the instability of perovskite materials greatly limits their applications in many fields, especially in biochemical detection [6-8]. Recently, many researchers have made advances towards the stabilization of perovskite materials [5, 9-13]. Wei et al. [14] successfully embedded perovskite in polystyrene microspheres for cell imaging applications. However, the large size of the microsphere limited the detection capabilities in aqueous solutions. Huang et al. [15] fabricated SiO_2 spheres coated perovskite without using water and catalyst, reported that the perovskite material exhibited greater stability in the presence of light and under aqueous conditions. A limitation of this method was the poor dispersion of the synthesized microspheres, thus making it unsuitable for biosensing applications. Hu et al. [16] encapsulated monodisperse perovskite nanoparticles with SiO_2 spheres, which significantly improved the stability of perovskite to water, air, and light, but these microspheres were not water-soluble. Therefore, it is highly desirable to establish a method for the synthesis of monodisperse, water-soluble, nanosized fluorescent perovskite microspheres.

It is well known that the monitoring of the hydrogen-ion concentration (such as pH) has profound significance in chemistry, biology, and environmental science fields [17-20]. Additionally, the pathology of many diseases is also closely related to the changes in pH inside the body. Abnormal pH values in cells can cause cellular disorder [21]. For example, the pH value of cancer cells is lower than that of normal cells [22, 23]. Therefore, the accurate and rapid monitoring of pH is of great significance for

physiological processes. At present, there are many methods to monitor pH value, such as electrochemical methods, surface-enhanced Raman spectroscopy, and fluorescence assays [24-26]. Among these methods, fluorescence assays are favored by many researchers owing to its superiority such as easy operation, rapid detection, low cost, and low interference from other sources.

Urea is mainly used in agriculture because of its high nitrogen content and low costs [27, 28]. In living organisms, it is produced mainly in the liver, dissolved in the blood, and eventually excreted through urine [29]. Urea abnormalities are indicative of some diseases, such as kidney failure, liver failure, and urinary tract obstruction [30, 31]. Therefore, detecting the urea content in urine and blood is an important means to prevent disease. Urease is a very important enzyme in soil; it can hydrolyze urea to $(NH_4)_2CO_3$ or NH_4HCO_3, and promote the absorption and utilization of crops [32]. Therefore, developing a fast, simple, and inexpensive method to detect urea and urease is the key problem to be urgently solved.

In this work, we first used a hot-injection method to prepare $CsPbBr_3$ perovskite quantum dots (CPQDs). These CPQDs were subsequently embedded in poly (styrene/acrylamide) (PS-PAA) microspheres using a swelling–shrinking method to successfully obtain water-soluble fluorescent perovskite microspheres (PDPS composites). Thus, a fluorescent sensing multifunctional system for monitoring the pH, urea and urease was established based on the prepared PDPS composites. Scheme 1 shows the specific detection principle. The pH detection system was mainly composed of PDPS composites and dopamine (DA). When the environment was acidic, the system showed strong fluorescence. However, as pH increased, more DA was oxidized to a quinone structure, leading to fluorescence quenching of the PDPS composites. Based on this principle, a fluorescent sensor was constructed to detect urea and urease. In the presence of urease, urea was hydrolyzed to ammonia, thereby

increasing the pH of the environment, subsequently leading to fluorescence quenching of the PDPS composites. Consequently, a fast, simple, high selectivity and sensitivity fluorescent probe was established for the simultaneous detection of pH, urea, and urease.

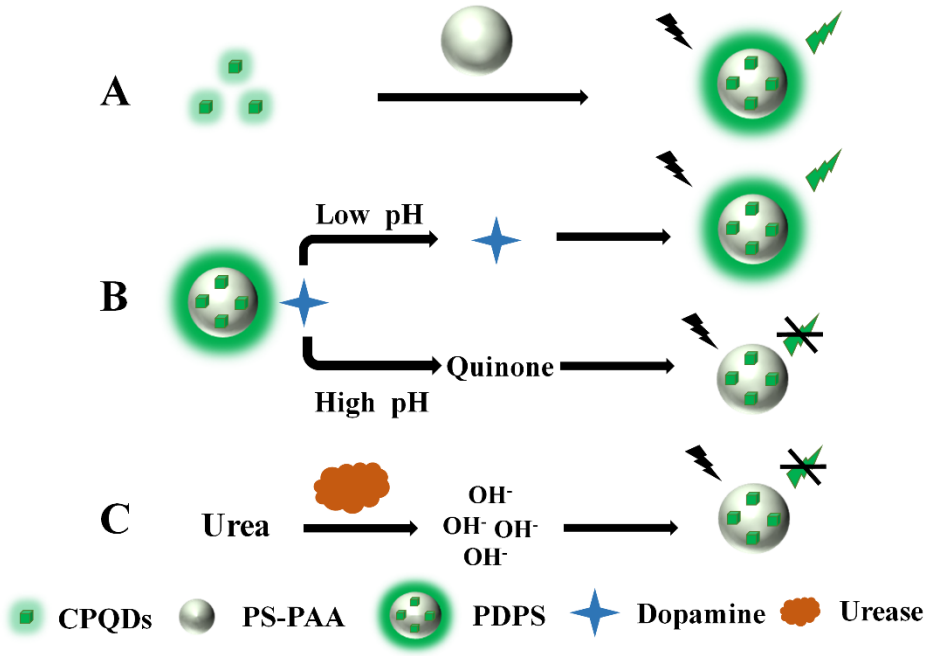

Scheme 1. Schematic diagram showing the formation of the PDPS composite fluorescence sensing platform. (A) CPQDs encapsulated in PS-PAA, (B) pH sensing principle, (C) the principle of urea and urease detection.

2. Material and methods

2.1 Instruments and measurements

Transmission electron microscopy (TEM) was performed using a Tecnai G2 F20 S-TWIN transmission electron microscope (FEI, USA) operated at an accelerating voltage of 200 kV. X-ray photoelectron spectroscopy (XPS) measurements were made on a ESCALAB250Xi spectrometer (ThermoFisher Scientific). Absorbance were recorded with BioTek Microplate Reader (ELx800, USA). Fluorescence measurements were obtained by using a Hitachi F-4700 fluorescence spectrometer (Hitachi. Ltd., Japan). X-ray diffraction (XRD) patterns were recorded on a XRD-6000 using Cu Kr radiation (λ=1.5418 Å) at

a step rate of 2° s^{-1}.

2.2 Materials

Cesium carbonate (Cs_2CO_3), lead(II) bromide ($PbBr_2$), 1-octadecene (ODE), oleic acid (OA) were purchased from Sigma-Aldrich. Dopamine hydrochloride, glycine (Gly), alanine (Ala), phenylalanine (Phe), histidine (His), glucose (Glu), threonine (Thr), and urea were purchased from Aldrich Chemical. Urease was purchased from Shanghai yuanye Bio-Technology Co., Ltd. NaCl, KCl, $MgCl_2$, and all other reagents were of analytical reagent grade. Nanopure water (18.2 MΩ; Millpore Co., USA) was used throughout the experiment. The serum and urine samples were obtained from ChongQing University Cancer Hospital.

2.3 Synthesis of $CsPbBr_3$

The preparation of CsPbBr3 were based on the previously reported procedures, with slight modifications and more rigorous controls of the experimental conditions for improved fluorescence properties[1, 2]. 0.0814 g of Cs_2CO_3, 4 mL of ODE and 250 μL of OA were added to a three-necked flask, heated to 120 °C, sealed and dried with nitrogen for 30 min. After the reaction, the temperature was raised to 150 °C until the powder was completely dissolved, then temperature was lowered to 125 °C before used 0.0676 g $PbBr_2$ and 5 mL ODE were added to a three-neck flask, heated to 120 °C, sealed and dried with nitrogen for 30min., 0.5 mLOA and 0.6 mL OLA were added, the reaction continued until the powder was completely dissolved and heated to 160 °C. Added 1 mL Cs-oleate precursor to the flask reacted 5 s and cooled in an ice bath.

The prepared sample was centrifuged at 12000 rpm for 5 min, and the precipitate was dispersed in 2 mL of n-hexane. The supernatant was collected by centrifugation, added 2 mL of toluene, 40 μL of OA and 4 mg of DDAB, the mixed solution was stirred at room temperature in the dark for 1 h. Excess ethyl

acetate was added to the sample after the reaction, and the mixture was centrifuged at 12000 rpm for 5 min. The precipitate was dispersed in 4 mL of toluene, centrifuged at 15000 rpm for 15 min, collected the supernatant. The $CsPbBr_3$ was stored at 4 °C.

2.4 Synthesis of PS-PAA

Preparation of PS-PAA [3]: Before the experiment, styrene was purified and concentrated by vacuum distillation, acrylamide and potassium persulfate were recrystallized in acetone and water respectively to purify the reagent. 100 mL of deionized water was added to a three flask, and heated to 70 °C in a N_2 atmosphere for 1 h. Then 10 mL purified styrene was added, after 5 min added 5 mL acrylamide-aqueous solution (0.4 g/mL), reacted 5 min added 5 mL potassium persulfate aqueous solution (80 mg/mL). The reaction continued for 15 h before filtering the product PS-PAA with absorbent cotton. The solution was centrifuged at 12000 rpm for 18 min, the supernatant was removed, and the precipitate was reldispersed in water. After repeated operations for 3 times, PS-PAA was finally dispersed in water and stored at 4 ºC.

Amination of PS-PAA: Prepared PS-PAA added to a round bottom flask and vigorously stirred. After being slowly heated to 50 ºC, 40 mL hydrazine hydrate was added. After reaction for 14 h, it was cooled to room temperature and dialyzed (8000-12000 Dalton) in ultrapure water for 7 days to obtain PS-PAA-NH_2.

Carboxylation of PS-PAA: The PS-PAA-NH2 was taken out and placed in a beaker, stirred at room temperature, and 3.0g succinic anhydride was added for several times. During the process, NaOH solution was used to adjust the pH of the system immediately, so that it remained pH around 4. After stirring for 2 h, the product was dialyzed in ultrapure water with dialysis bag (8000-12000 Dalton) for 7 days to obtain PS-PAA-COOH.

2.5 Preparation of the PDPS composites [33]

The appropriate amount of PS-PAA solution (1 mL) was centrifuged at 14,000 rpm for 15 min. The precipitate obtained was dispersed in ethanol and then centrifuged again to remove the supernatant. Next, the precipitate was dispersed in 900 μL of isopropanol. Then 100 μL of CPQDs was added and the solution was sonicated for 30 min. After the reaction, an excess of n-hexane was added to the mixture and centrifuged at 1000 rpm for 1 min to remove the supernatant. The resultant precipitate was washed two times with water and ethanol, and dispersed in water, then stored at 4 °C.

2.6 pH sensing

The pH sensing platform was designed using the following protocol: 10 μL of the PDPS composites and 20 μL of DA were added to a 600 μL Britton-Robison (BR) buffer solution at various pH values. After being evenly mixed, the PDPS composites were incubated at 37 °C for 30 min. Fluorescence spectra were then obtained in the wavelength range of 470–570 nm with the excitation wavelength set at 300 nm.

2.7 Detection of Urea

For the detection of urea, the PDPS composites were first dispersed in a phosphate buffer (PB) solution (pH 6.8, 0.01 M).Then, 50 μL of DA (25 mM), 5 μL of urease (1.25 U/mL) and 45 μL of urea solutions at different concentrations (0.00167, 0.0083, 0.0167, 0.0833, 0.167, 0.5, 0.833, 1.667, 3.33, 5, 6.667, 8.333, 16.67 mM) were added to the 200 μL of PDPS composites in centrifugal tubes. The solutions were incubated for 30 min at 37 °C, and fluorescence spectra were then obtained from 470–570 nm at an excitation wavelength of 300 nm. The selectivity of this sensing system for urea was assessed in the presence of cations (such as K+, Na+, and Mg2+) and amino acids (such as Ala, Phe, His, Glu, Gly, and Thr).

2.8 Detection of Urease

For urease detection, the PDPS composites were first dispersed in the PB buffer solution (pH 6.8, 0.01 M). Then, 50 μL of DA (25 mM), 45 μL urea solution (0.05 M), and 5 μL of urease at different concentrations (0.0021, 0.0042, 0.0208, 0.0416, 0.0833, 0.1333, 0.2, 0.2667, 0.3125, 0.333, 0.4, 0.433, 0.5, 0.667, 0.833, 1, 1.25 U/mL) were added to the 200 μL PDPS samples. After the mixture was thoroughly mixed, the samples were incubated at 37 °C for 30 min, and fluorescence spectra were then obtained from 470–570 nm at an excitation wavelength of 300 nm.

2.9 Real serum samples assay

To verify the feasibility of the PDPS composites based sensing system for the detection of urea, serum samples were employed. The serum samples were diluted 50-fold with the PB buffer solution (pH 6.8, 0.01 M), and urea of different concentrations was added to prepare the spiked samples.

3 Results and discussion

3.1 Characterization of PDPS composites

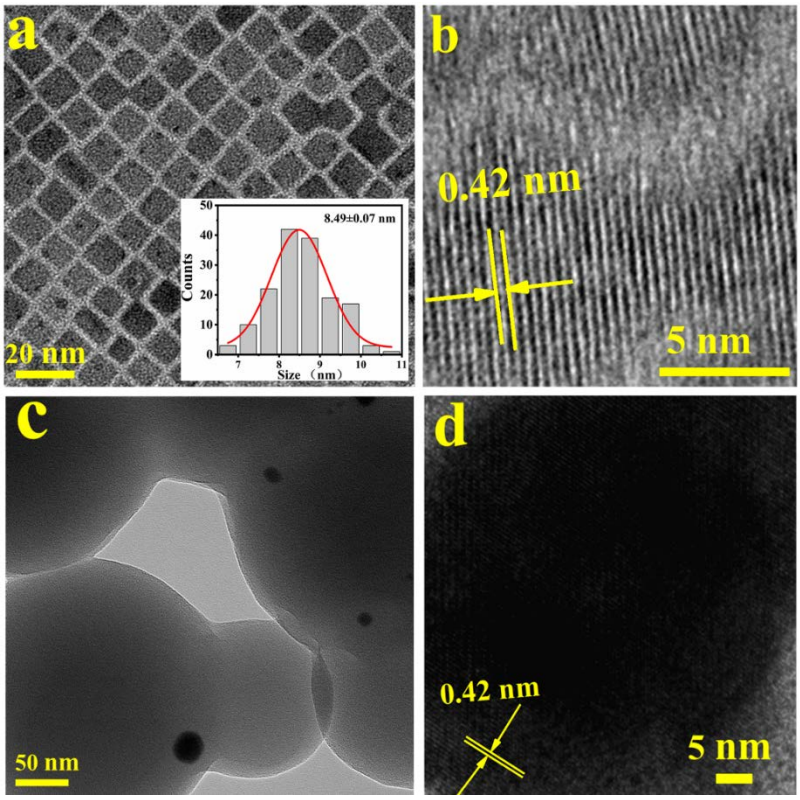

Fig. 1. (a) TEM image of CPQDs, (b) HRTEM image of a single CPQDs, (c) TEM image of the prepared PDPS composites, and (d) HRTEM image of the PDPS composites.

There are many preparation methods for $CsPbBr_3$ perovskite quantum dots (CPQDs), but those based on the hot-injection method usually have a more uniform particle size and better optical stability. As a result, CPQDs were prepared by the hot-injection method. Fig. 1a-b shows the prepared CPQDs with an average particle size of 8.49 nm, and a lattice spacing of 0.42 nm. The CPQDs were subsequently embedded in polystyrene and poly (acrylic acid) (PS-PAA) microspheres using a swelling–shrinking method. These PS-PAA microspheres had special internal hydrophobic and external hydrophilic characteristics, which enabled the perovskite materials to maintain stable fluorescence characteristics internally and also have good water dispersion. The prepared PS-PAA microspheres were characterized by TEM (Fig. S1a-b), which showed that the average diameter of PS-PAA was 285 nm. Fig. 1c-d shows the TEM images of the PDPS composites. It is clearly found that the lattice spacing of the embedded CPQDs remains constant, which suggested that CPQDs were successfully embedded in the PS-PAA microspheres without changing the crystal structure.

In order to further prove that $CsPbBr_3$ perovskite quantum dots was successfully encapsulated in PS-PAA microspheres, SEM/EDX elemental mapping analysis and TEM/EDX elemental mapping analysis were performed on PDPS composites, respectively. It is difficult to observe some element distribution in the Fig. S2, maybe attribute to $CsPbBr_3$ perovskite quantum dots was encapsulated in PS-PAA microspheres or the particle size of $CsPbBr_3$ perovskite quantum dots were too small, results these signals were difficult to be detected by SEM analysis. Therefore, TEM was further performed to analyze the element distribution. As is seen in Fig. S4, there are some nanometer particles seen in inner of PDPS composites in the HAADF-STEM image, and the corresponding energy dispersive spectrum (EDS)

layered images show that PDPS composites are composed of C, O, N, Cs, Pb and Br elements. In conclusion, the above characterization results have proved the successful preparation of PDPS composites.

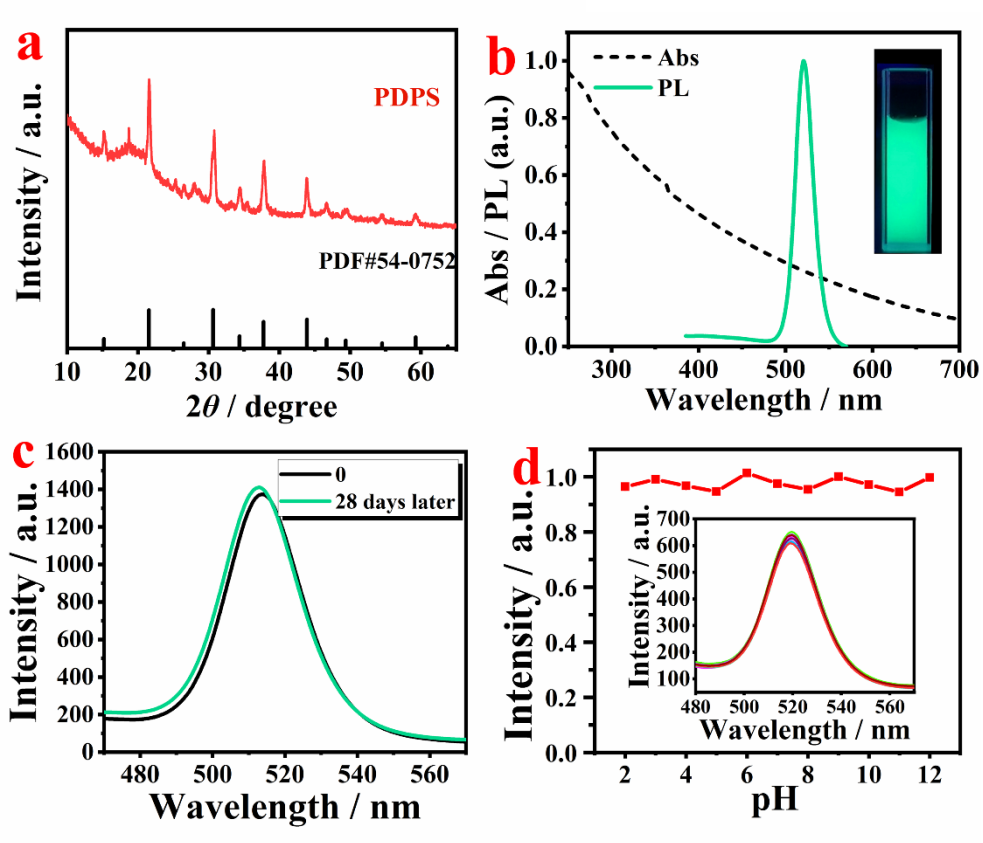

Fig. 2 (a) XRD patterns of the prepared PDPS composites, (b) Fluorescent emission spectra (green line) and absorbance spectra (black line) of the PDPS composites. The inset photograph shows a strong green PL emission under UV light (λ = 365 nm), (c) Storage stability in aqueous solution, and (d) PL stability in buffer solutions at various pH values.

Similarly, the XRD results (Fig. 2a) also showed that the diffraction peaks of the PDPS composites fluorescent microspheres were matched with the CPQDs. The result showd that the wrapping process did not change the crystal structure of the CPQDs, further proving the successful preparation of the PDPS composites. Fig. 2b represents the optical characterization of the PDPS composites. The emission wavelength of the PDPS composites was 519 nm. No obvious absorption peak was observed in the

absorption spectrum but green fluorescence was observed under UV light (inset in Fig. 2b). To verify the photoluminescence (PL) stability of the PDPS composites, the samples were dispersed in aqueous solution and their fluorescence characteristics were tested after 28 days. Fig. 2c shows that the fluorescence intensity change of the sample was almost negligible even after 28 days, indicating that the prepared PDPS composites had ultra-stable fluorescence characteristics. At the same time, the sample was dispersed in buffer solutions at different pH values. The results showed (Fig. 2d) that the fluorescence intensity of the PDPS composites was very consistent under different pH conditions. In conclusion, all of the above results proved that PDPS composites had good PL stability in aqueous environments, promoting their sustainable utilization in biological detection.

3.2 Fluorescence response of the PDPS composites to pH

The PDPS composites with DA were employed to establish a pH sensing system. As seen in Fig. 3a-b, the fluorescence intensity of the PDPS composites was almost unchanged in the pH range of 2-4. However, at higher pH values, DA was oxidized to quinone. Quinone, on account of its good electron accepting properties, caused the fluorescence quenching of the PDPS composites [34, 35]. As shown in Fig. 2d, in the pH range of 2 to 12, the fluorescence of the PDPS composites remained almost unchanged in the absence of dopamine, indicating the stability of the PDPS composites in this pH range. Therefore, we constructed a novel method to modify the as-prepared PDPS composites with dopamine, which broke the fluorescence intensity balance of the PDPS composites in environments at different pH values. The presence of DA facilitated the fluorescence quenching of the PDPS composites. To verify the response time of the PDPS composites at different pH value, the PDPS composites were dispersed in BR buffer solutions with pH values of 3 and 9. The fluorescence intensity was recorded for different reaction times. It was observed that the fluorescence intensity of the PDPS composites remained unchanged until 30 min

(Fig. S5), indicating that the reaction was complete, so the optimal reaction time was 30 min. It can be seen from Fig. S6 that for different concentrations of DA the linear relationship between the fluorescence intensity and the DA concentration was different. When the DA concentration was 0.6 mM, as shown in Fig. 3b, and the pH was in the range of 4-12, the fluorescence intensity and pH value showed a good linear relationship (R^2=0.994). Therefore, 0.6 mM DA appeared to be the optimized concentration for pH sensing applications.

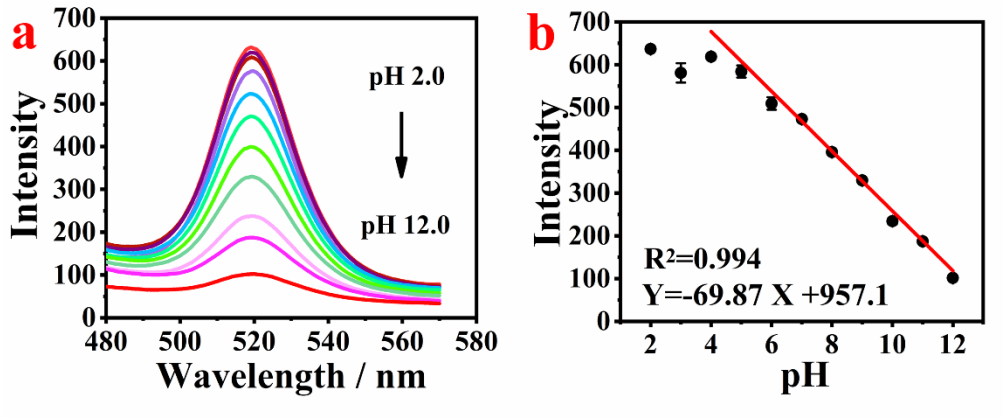

Fig. 3 (a) Fluorescent emission spectra (λex=300 nm) of PDPS/DA at different pH value. (b) The linear relationship between the fluorescence intensity at various pH values.

3.3 Detection of Urea/Urease

Motivated by the response of the PDPS composite fluorescent sensor to different pH values, we used the system to detect urea and urease. As we know, urea can be hydrolyzed in the presence of urease according to Eq. (1) [36]

$$Urea + H_2O \xrightarrow{\text{Urease}} HCO_3^- + OH^- + 2NH_4^+ \quad (1)$$

The generated OH^- can change the pH value and then oxidize DA to generate a quinone structure, thereby causing fluorescence quenching of the PDPS composites, and achieving the purpose of detecting urea and urease. In order to further confirm the sensing capability of the composite in physiologically active systems, the influence of different concentrations of interfering substance on the fluorescence of the

PDPS composites were studied. As evident from Fig. S7a-b, there was no fluorescence quenching of the PDPS composites when in the presence of urea, urease, NH_4^+ or HCO_3^- in the environment. In order to use this system to accurately detect urea, it was also imperative to regulate the concentration of DA and urease. As shown in Fig. S8a-c, to detect urea the optimal DA concentration was determined to be 4.1 mM, the optimal urease concentration was 1.25 U/mL and the optimal temperature was 37 °C.

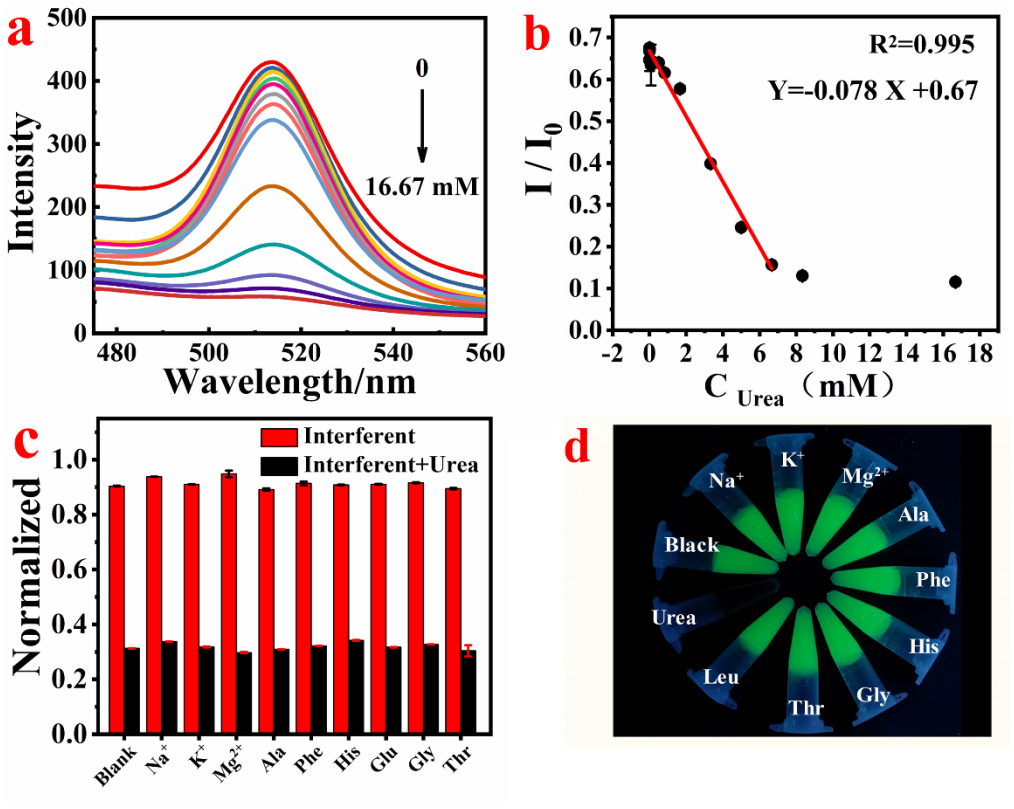

Fig. 4 (a) Fluorescent emission spectra (λex=300 nm) of the PDPS composites with different concentrations of urea. (b) The linear relationship with error bars for urea detection. (c) Interference studies of the PDPS composites sensor towards urea. (d) FL images of the aqueous suspension of the PDPS composites to different interfering substances, excited by a 365 nm of UV-lamp.

The PDPS/DA sensing system was used to detect different concentrations of urea (Fig.4a-b). As the urea concentration continuously increased, the fluorescence intensity of the PDPS composites gradually decreased. The quenching can be expressed with Stern–Volmer equation:

$$\frac{I_0}{I} = 1 + K_{SV}[c] \quad (2)$$

Where I_0 and I are the fluorescence intensities in the absence and presence of urea, [c] is the concentration of urea and K_{sv} is the quenching constants, which can reflect the sensitivity of the sensor. In this study, as shown in Fig. S9, at low concentrations there was a linear relationship between (I_0/I-1) and urea concentration, but when urea concentration increases, there was no linear relationship. Thus, the quenching mechanism of urea were dynamic and static fluorescence quenching. Through calculation, the K_{sv} of urea is 292.5 M^{-1}. The fluorescent sensor showed a good linear relationship in the urea concentration range of 1.67 μM-6.67 mM (Y= -0.078 [C_{urea}] +0.67, R^2=0.995). Therefore, the detection limit of urea was 1.67 μM. To further demonstrate the selectivity of the system for urea detection, we tested some substances for their potentially interference (Na^+, K^+, Mg^{2+}, Ala, Phe, His, Gly, Thr and Leu) under the same conditions. The interference studies against cations and amino acids are shown in Fig.4 c. The red bars were the effect of different interference materials on the fluorescence intensity of the PDPS composites, and the black bars verified that after joining the interference materials, urea influenced the fluorescence intensity of the PDPS composites. As evident from Figure 4c, the interference studies exhibited no obvious influence on the sensing system; thus, the system could be successfully employed for the detection of urea. Fig. 4d shows a photograph of different interfering substances added to the PDPS composites under a UV lamp (λ ex=365 nm). The fluorescence intensity of the PDPS composites was not affected by any interfering substances, except for urea, when compared with the blank group. Furthermore, comparing this urea detection sensing system with the previous method [27, 28, 31, 37-40], it was found that this sensing system had obvious advantages in regard to response time and detection limit (Table. S1). The sensing system reported here is robust and applicable for detecting urea in physiologically active biofluids.

Similarly, in order to detect urease at different concentrations, we fixed the added urea concentration to 0.05 M. Fig. 5a shows that as the urease concentration increases the fluorescence intensity of the PDPS composites slowly decreases. Through used Stern–Volmer equation calculation, the K_{sv} of urease is 106.5 mL/U. As shown in Fig. S10, the results presented are similar to those of urea detection, thus the quenching mechanism of urease were also dynamic and static fluorescence quenching. When the urease concentration was between 2.1-550 mU/mL (Fig. 5b) the fluorescent sensor showed a good linear relationship (Y= -1.22 [C_{urease}] +0.816, R^2=0.985). The limit detection of the urease sensing system was 2.1 mU/mL. Compared with existing method (Table. S2), our method shows excellent reliability and stability.

Compared with existing method (Table. S2), our method shows excellent reliability and stability. Most of the reported perovskite-based sensors are detected in the oil phase, which is not conducive to the application of biochemical detection. More importantly, the constructed detection method has the advantages of easy operation, rapid response and can detect in water, indicating that this method has great reliability and potential in detection urea and urease in real samples.

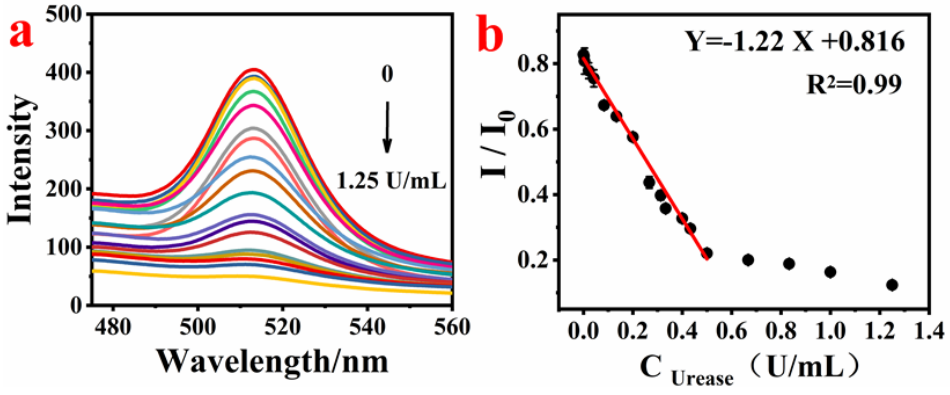

Fig. 5 (a) Fluorescent emission spectra (λex=300 nm) of the PDPS composites with different concentrations of urease. (b) The linear relationship with error bar for urease detection.

3.4 Detection in real samples

We tested the urea content in real human serum and urine samples by employing the standard addition method to evaluate the feasibility of the system in real samples. From the results in Table 1, we can see that the recovery for the three different samples in human serum and urine were 91.7-112% and 98-100.8%, respectively, and the RSDs ≤ 7%. The Recovery could be calculated according to the Equation, Recovery % = 100% × (Detected concentration/Added concentration) [41, 42]. The fluorescence spectra of the PDPS composites with different concentrations of urea in real human serum and urine samples are displayed in Fig. S11 and Fig. S12. According to the previous studies [43, 44], the unknown concentration of human serum and urine was quantified as 29 mM and 4.21 mM, respectively(Fig. S13 and Fig. S14). The above results show that this fluorescence detection sensing system has excellent potential for sensing urea in real serum samples.

Table 1

Detection of urea in real human samples.

sample	Urea added (mM)	Urea found (mM)	Recovery (%)	RSD (%, n=3)
Human	0.50	0.56±0.04	112.0	7.0
Serum	1.33	1.43±0.09	107.0	6.0
	6.67	6.12±0.03	91.7	0.5
Human	0.50	0.49±0.01	98.0	2.0
urine	1.33	1.34±0.02	100.8	1.5
	6.67	6.68±0.05	100.1	0.7

4 Conclusion

In this work, CPQDs were embedded in PS-PAA microspheres using a swelling–shrinking method to construct PDPS composites. These composites exhibited high stability over longterm exposure to air

and aqueous solutions. The biocompatible PDPS composites reported here could be used for the accurate and rapid monitoring of pH changes in a biological system. Moreover, this system could be easily extended to clinical applications such as monitoring pH in tumour microenvironments and new drug delivery systems. The PDPS composites could also be successfully employed for the detection of urea and urease with high sensitivity and selectivity in real clinical samples.

5 Declarations

Funding

This work is supported by the Chongqing Entrepreneurship and Innovation Support Program (CX201803), the China Fundamental Research Funds for the Central Universities (Grant No. 2019CDQYGD020, 2019CDCGGD304 and 2020CDJGFCG006), and the National Key Research and Development Program of China (Grant No. 2016YFC0101100 and 2016YFE0125200).

Acknowledgment

Thanks are given to the Analytical and Testing Center of Chongqing University and Beijing Zhongkebaice Technology Service Co., Ltd for providing the test platform.

Ethics approval

The study was approved by the medical ethical committee (ChongQing University Cancer Hospital. No. CZLS2020259-A).

Conflict of interest

The authors declare that they have no conflict of interest.

Consent for publication

All the authors and participants consent to the publication of this manuscript in Analytical and Bioanalytical Chemistry.

Appendix A. Supplementary data

Supplementary data related to this article are enclosed as a separate file.

References:

1. Raju TD, Veeralingam S, Badhulika S. Polyvinylidene Fluoride/ZnSnO3 Nanocube/Co3O4 Nanoparticle Thermoplastic Composites for Ultrasound-Assisted Piezo-Catalytic Dye Degradation. ACS Applied Nano Materials. 2020;3(5):4777-87. http://doi:10.1021/acsanm.0c00771.

2. Protesescu L, Yakunin S, Bodnarchuk MI, Krieg F, Caputo R, Hendon CH et al. Nanocrystals of Cesium Lead Halide Perovskites (CsPbX3, X = Cl, Br, and I): Novel Optoelectronic Materials Showing Bright Emission with Wide Color Gamut. Nano Letters. 2015;15(6):3692-6. http://doi:10.1021/nl5048779.

3. Dai J, Xi J, Zu Y, Li L, Xu J, Shi Y et al. Surface mediated ligands addressing bottleneck of room-temperature synthesized inorganic perovskite nanocrystals toward efficient light-emitting diodes. Nano Energy. 2020;70:104467. http://doi:10.1016/j.nanoen.2020.104467.

4. Yang W, Fei L, Gao F, Liu W, Xu H, Yang L et al. Thermal polymerization synthesis of CsPbBr3 perovskite-quantum-dots@copolymer composite: Towards long-term stability and optical phosphor application. Chemical Engineering Journal. 2020;387:124180. http://doi:10.1016/j.cej.2020.124180.

5. Wang F, Wang H, Ali A, Zhang Y, Cui X, Liu Y. In-situ one-step electrospray fabrication of polyvinylidene fluoride encapsulated CsPbBr3 spheres with high stability and cell imaging application. Inorganic Chemistry Communications. 2019;106:99-103. http://doi:10.1016/j.inoche.2019.05.032.

6. Chen Y, Yu M, Ye S, Song J, Qu J. All-inorganic CsPbBr3 perovskite quantum dots embedded in dual-mesoporous silica with moisture resistance for two-photon-pumped plasmonic nanoLasers. Nanoscale. 2018;10(14):6704-11. http://doi:10.1039/c7nr08670a.

7. Huang S, Wang B, Zhang Q, Li Z, Shan A, Li L. Postsynthesis Potassium-Modification Method to Improve Stability of CsPbBr3 Perovskite Nanocrystals. Advanced Optical Materials. 2018;6(6):1701106. http://doi:10.1002/adom.201701106.

8. Zhang W, Ye Y, Liu C, Zhao Z, Wang J, Han J et al. Revealing the Effects of Defects on Ultrafast Carrier Dynamics of CsPbI3 Nanocrystals in Glass. The Journal of Physical Chemistry C. 2019;123(25):15851-8. http://doi:10.1021/acs.jpcc.9b03901.

9. Huang S, Zhang T, Jiang C, Qi R, Luo C, Chen Y et al. Luminescent CH3NH3PbBr3/β‐Cyclodextrin Core/Shell Nanodots with Controlled Size and Ultrastability through Host‐Guest Interactions. ChemNanoMat. 2019;5(10):1311-6. http://doi:10.1002/cnma.201900381.

10. Pan A, Wu Y, Yan K, Yu Y, Jurow MJ, Ren B et al. Stable Luminous Nanocomposites of Confined Mn(2+)-Doped Lead Halide Perovskite Nanocrystals in Mesoporous Silica Nanospheres as Orange Fluorophores. Inorg Chem. 2019;58(6):3950-8. http://doi:10.1021/acs.inorgchem.9b00010.

11. Wei Z, Chen Y, Lin P, Yan Q, Fan Y, Cheng Z. Synthesis and encapsulation of all inorganic perovskite nanocrystals by microfluidics. Journal of Materials Science. 2019;54(9):6841-52. http://doi:10.1007/s10853-019-03397-9.

12. Wu H, Lin S, Wang R, You X, Chi Y. Water-stable and ion exchange-free inorganic perovskite quantum dots encapsulated in solid paraffin and their application in light emitting diodes. Nanoscale. 2019;11(12):5557-63. http://doi:10.1039/c8nr09384a.

13. Lv W, Li L, Xu M, Hong J, Tang X, Xu L et al. Improving the Stability of Metal Halide Perovskite

Quantum Dots by Encapsulation. Adv Mater. 2019;31(28):e1900682. http://doi:10.1002/adma.201900682.
14. Wei Y, Deng X, Xie Z, Cai X, Liang S, Ma Pa et al. Enhancing the Stability of Perovskite Quantum Dots by Encapsulation in Crosslinked Polystyrene Beads via a Swelling-Shrinking Strategy toward Superior Water Resistance. Advanced Functional Materials. 2017;27(39):1703535. http://doi:10.1002/adfm.201703535.
15. Huang S, Li Z, Kong L, Zhu N, Shan A, Li L. Enhancing the Stability of CH3NH3PbBr3 Quantum Dots by Embedding in Silica Spheres Derived from Tetramethyl Orthosilicate in "Waterless" Toluene. J Am Chem Soc. 2016;138(18):5749-52. http://doi:10.1021/jacs.5b13101.
16. Hu H, Wu L, Tan Y, Zhong Q, Chen M, Qiu Y et al. Interfacial Synthesis of Highly Stable CsPbX3/Oxide Janus Nanoparticles. J Am Chem Soc. 2018;140(1):406-12. http://doi:10.1021/jacs.7b11003.
17. Gao P, Li M, Zhang Y, Dong C, Zhang G, Shi L et al. Facile, rapid one-pot synthesis of multifunctional gold nanoclusters for cell imaging, hydrogen sulfide detection and pH sensing. Talanta. 2019;197:1-11. http://doi:10.1016/j.talanta.2018.12.078.
18. Staudinger C, Strobl M, Breininger J, Klimant I, Borisov SM. Fast and stable optical pH sensor materials for oceanographic applications. Sensors and Actuators B: Chemical. 2019;282:204-17. http://doi:10.1016/j.snb.2018.11.048.
19. Zhao C, Li X, Cheng C, Yang Y. Green and microwave-assisted synthesis of carbon dots and application for visual detection of cobalt(II) ions and pH sensing. Microchemical Journal. 2019;147:183-90. http://doi:10.1016/j.microc.2019.03.029.
20. Liu J, Wang H, Guo M, Li L, Chen M, Jiang S et al. Extract from Lycium ruthenicum Murr. Incorporating κ-carrageenan colorimetric film with a wide pH–sensing range for food freshness monitoring. Food Hydrocolloids. 2019;94:1-10. http://doi:10.1016/j.foodhyd.2019.03.008.
21. Zhang J, Li J, Chen B, Kan J, Jiang T, Zhang W et al. An off-on fluorescent probe for real-time sensing the fluctuations of intracellular pH values in biological processes. Dyes and Pigments. 2019;170:107620. http://doi:10.1016/j.dyepig.2019.107620.
22. Georgiev NI, Said AI, Toshkova RA, Tzoneva RD, Bojinov VB. A novel water-soluble perylenetetracarboxylic diimide as a fluorescent pH probe: Chemosensing, biocompatibility and cell imaging. Dyes and Pigments. 2019;160:28-36. http://doi:10.1016/j.dyepig.2018.07.048.
23. Yu K-K, Tseng W-B, Wu M-J, Alagarsamy ASKK, Tseng W-L, Lin P-C. Polyadenosine-based fluorescent probe for reversible pH sensing based on protonated adenine-adenine base pairs: Applications to sensing of enzyme-substrate system and enzymatic logic gates. Sensors and Actuators B: Chemical. 2018;273:681-8. http://doi:10.1016/j.snb.2018.06.116.
24. Ghoneim MT, Nguyen A, Dereje N, Huang J, Moore GC, Murzynowski PJ et al. Recent Progress in Electrochemical pH-Sensing Materials and Configurations for Biomedical Applications. Chem Rev. 2019;119(8):5248-97. http://doi:10.1021/acs.chemrev.8b00655.
25. Zhang Z, Bando K, Mochizuki K, Taguchi A, Fujita K, Kawata S. Quantitative Evaluation of Surface-Enhanced Raman Scattering Nanoparticles for Intracellular pH Sensing at a Single Particle Level. Anal Chem. 2019;91(5):3254-62. http://doi:10.1021/acs.analchem.8b03276.
26. Panda BR, Chattopadhyay A. A water-soluble polythiophene-Au nanoparticle composite for pH sensing. J Colloid Interface Sci. 2007;316(2):962-7. http://doi:10.1016/j.jcis.2007.08.033.
27. Huang H, Li J, Liu M, Wang Z, Wang B, Li M et al. pH-controlled fluorescence changes in a novel semiconducting polymer dot/pyrogallic acid system and a multifunctional sensing strategy for urea,

urease, and pesticides. Analytical Methods. 2017;9(47):6669-74. http://doi:10.1039/c7ay02284k.
28. Zhang F, Wang M, Zhang L, Su X. Ratiometric fluorescence system for pH sensing and urea detection based on MoS2 quantum dots and 2, 3-diaminophenazine. Anal Chim Acta. 2019;1077:200-7. http://doi:10.1016/j.aca.2019.06.001.
29. Pundir CS, Jakhar S, Narwal V. Determination of urea with special emphasis on biosensors: A review. Biosens Bioelectron. 2019;123:36-50. http://doi:10.1016/j.bios.2018.09.067.
30. Liu S, Shi F, Chen L, Su X. Dopamine functionalized CuInS2 quantum dots as a fluorescence probe for urea. Sensors and Actuators B: Chemical. 2014;191:246-51. http://doi:10.1016/j.snb.2013.09.056.
31. Rafiq K, Mai HD, Kim JK, Woo JM, Moon BM, Park CH et al. Fabrication of a highly effective electrochemical urea sensing platform based on urease-immobilized silk fibroin scaffold and aminated glassy carbon electrode. Sensors and Actuators B: Chemical. 2017;251:472-80. http://doi:10.1016/j.snb.2017.05.048.
32. Jannah F, Kim J-M. pH-sensitive colorimetric polydiacetylene vesicles for urease sensing. Dyes and Pigments. 2019;169:15-21. http://doi:10.1016/j.dyepig.2019.04.072.
33. Chen M, An J, Hu Y, Chen R, Lyu Y, Hu N et al. Swelling-shrinking modified hyperstatic hydrophilic perovskite polymer fluorescent beads for Fe(III) detection. Sensors and Actuators B: Chemical. 2020;325:128809. http://doi:10.1016/j.snb.2020.128809.
34. Medintz IL, Stewart MH, Trammell SA, Susumu K, Delehanty JB, Mei BC et al. Quantum-dot/dopamine bioconjugates function as redox coupled assemblies for in vitro and intracellular pH sensing. Nat Mater. 2010;9(8):676-84. http://doi:10.1038/nmat2811.
35. Ji X, Palui G, Avellini T, Na HB, Yi C, Knappenberger KL, Jr. et al. On the pH-dependent quenching of quantum dot photoluminescence by redox active dopamine. J Am Chem Soc. 2012;134(13):6006-17. http://doi:10.1021/ja300724x.
36. Moynihan HJ, Lee CK, Clark W, Wang N-HL. Urea Hydrolysis by Immobilized Urease in a Fixed-Bed Reactor: Analysis and Kinetic Parameter Estimation. Biotechnology and Bioengineering. 1989;34(7):951-63.
37. Ibrahim AA, Ahmad R, Umar A, Al-Assiri MS, Al-Salami AE, Kumar R et al. Two-dimensional ytterbium oxide nanodisks based biosensor for selective detection of urea. Biosens Bioelectron. 2017;98:254-60. http://doi:10.1016/j.bios.2017.06.015.
38. Deng HH, Zheng XQ, Wu YY, Shi XQ, Lin XL, Xia XH et al. Alkaline peroxidase activity of cupric oxide nanoparticles and its modulation by ammonia. Analyst. 2017;142(20):3986-92. http://doi:10.1039/c7an01293d.
39. Hassan RYA, Kamel AM, Hashem MS, Hassan HNA, Abd El-Ghaffar MA. A new disposable biosensor platform: carbon nanotube/poly(o-toluidine) nanocomposite for direct biosensing of urea. J Solid State Electrochem. 2018;22(6):1817-23. http://doi:10.1007/s10008-017-3857-z.
40. Oymak T, Ertaş N, Tamer U. Use of Water Soluble and Phosphorescent MPA Capped CdTe Quantum Dots for Detection of Urea. The Turkish Journal of Pharmaceutical Sciences. 2018;15(1):44-9. http://doi:10.4274/tjps.02986.
41. Rong M, Feng Y, Wang Y, Chen X. One-pot solid phase pyrolysis synthesis of nitrogen-doped carbon dots for Fe3+ sensing and bioimaging. Sensors and Actuators B: Chemical. 2017;245:868-74. http://doi:10.1016/j.snb.2017.02.014.
42. Ma J, Zhang H, Peng F, Yang X, Li ZL, Sun L et al. Carbon dots as fluorescent nanoprobe for the determination of N-acetyl-beta-d-glucosaminidase activity. Anal Chim Acta. 2020;1101:129-34. http://doi:10.1016/j.aca.2019.12.018.

469 43. Veeralingam S, Badhulika S. Surface functionalized β-Bi2O3 nanofibers based flexible, field-effect
470 transistor-biosensor (BioFET) for rapid, label-free detection of serotonin in biological fluids. Sensors
471 and Actuators B: Chemical. 2020;321:128540. http://doi:10.1016/j.snb.2020.128540.
472 44. Sushmitha Veeralingam SK, and Sushmee Badhulika. AI/ML-Enabled 2-D - RuS2 Nanomaterial-
473 Based Multifunctional, Low Cost,Wearable Sensor Platform for Non-Invasive Point of Care Diagnostics.
474 IEEE Sens J. 2020;20(15):8437-44. http://doi:10.1109/JSEN.2020.2984807.

475